GAS-LIQUID FLOW AROUND AN OBSTACLE IN A VERTICAL PIPE - EXPERIMENTS AND CFD SIMULATION

H.-M. Prasser[1], T. Frank[2], M. Beyer[1], H. Carl[1], H. Pietruske[1], P. Schütz[1]

[1] Forschungszentrum Rossendorf. e.V., PSF 510119, 01314 Dresden, prasser@fz-rossendorf.de
[2] ANSYS Germany, Staudenfeldweg 12, 83624 Otterfing, E-mail: Thomas.Frank@ansys.com

1. Introduction

In the frame of the TOPFLOW project, vertical pipe flow is experimentally studied in order to develop and validate models for bubble forces as well as for bubble coalescence and fragmentation in a gas-liquid two-phase flow. The advantage of TOPFLOW [1] consists in the combination of (1) a large scale of the test channel with (2) a wide operational range both in terms of the superficial velocities and the system pressure and finally (3) the availability of an instrumentation that is capable in resolving structures of the gas-liquid interface, namely the wire-mesh sensors.

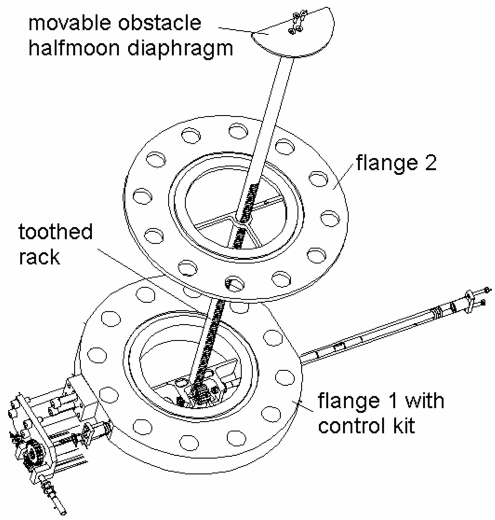

Fig. 2: Movable obstacle with drive support for TOPFLOW

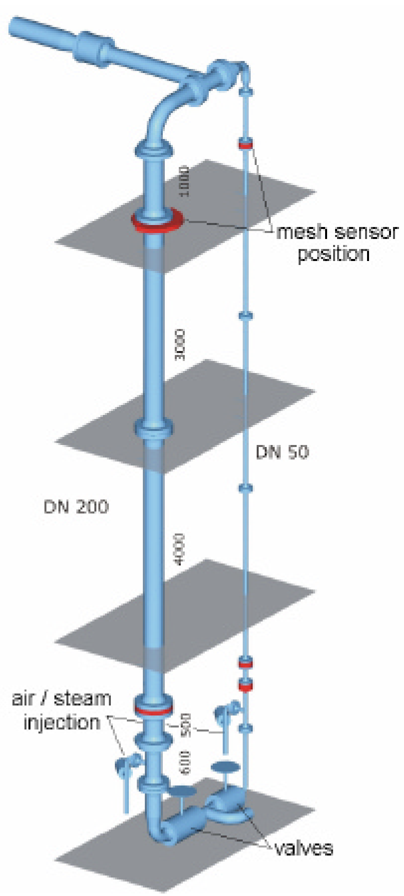

Fig. 1: Vertical test section DN200 of TOPFLOW

After a large number of experiments in plain vertical pipes [2-5], which are the basis of the development for a multi-bubble size model for ANSYS CFX 10.0, the large test section with a nominal diameter of DN200 (Fig. 1) was used to study the flow field around an asymmetric obstacle (Fig. 2). This is an ideal test case for the CFD code validation, since the obstacle creates a pronounced three-dimensional two-phase flow field. Curved stream lines, which form significant angles with the gravity vector, a recirculation zone in the wake and a flow separation at the edge of the obstacle are phenomena widespread in real industrial components and installations. It has to be shown that the CFD-code predicts these phenomena well, after it has been equipped by new models, developed in simpler experimental geometries.

Recently, test series were performed with an air-water flow at ambient conditions as well as with a steam-water mixture at a saturation pressure of 6.5 MPa. Before the experiments were commissioned, an ANSYS CFX 10.0 pre-test calculation was carried out for one of the experimental tests.

2. Test arrangement

The test pipe has an inner diameter of 195.3 mm and a total height of 9 m. Water is supplied from the bottom with a maximum flow rate of 50 kg/s. The two-phase flow is generated by feeding gas through an injector consisting of 16 radial tubes with a total number of 152 orifices of 0.8 mm diameter, connected to a conical head placed in the centre of the pipe (Fig. 3). The diaphragm (Fig. 2) has is a half-moon shaped disk, the straight edge of which is arranged along the diameter of the pipe,

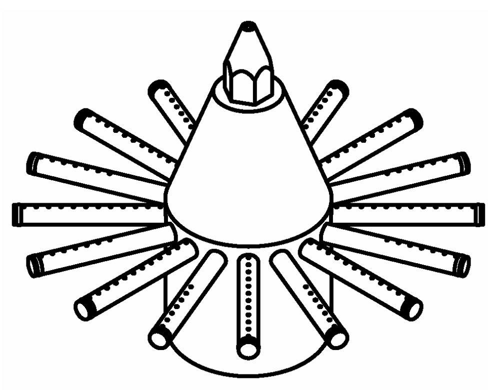

Fig. 3: Gas injection head

while the circular edge is in a distance of 10 mm from the inner wall of the pipe. The disk is mounted on top of a toothed rod connected to a translation mechanism to change the axial position of the diaphragm.

Both obstacle and moving mechanism can be inverted and mounted either upstream or downstream of the wire-mesh sensor shown in Fig. 4. The sensor was located 6.17m downstream of the gas injection, when the asymmetric obstacle was put upstream of the sensor. When the obstacle was put downstream of the sensor, the distance was 5.11 m. The described arrangement allows to acquire local instantaneous void fractions from the full cross-section of the pipe with a spatial resolution of 3 mm and a rate of 2.5 kHz within the three-dimensional flow field around the diaphragm. The distance between sensor and diaphragm can be varied from 10 mm to a maximum distance of 520 mm without moving the sensor position, which is essential to perform high-pressure experiments in an efficient way, i.e. without dismantling and rearranging the test facility each time the measuring position has to be changed.

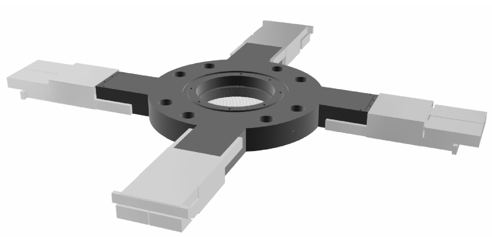

Fig. 4: High-pressure wire-mesh sensor (DN200), measuring matrix of 64x64 points [6]

3. Test parameters

Measurements were carried out with an air-water flow at ambient pressure and a temperature of 25 °C as well as with a steam-water mixture under saturation conditions at 6.5 MPa for the superficial velocities shown in Fig. 5. The following distances between diaphragm and mesh sensors were realized: $\Delta z = \pm 520, \pm 250, \pm 160, \pm 80, \pm 40, \pm 20, \pm 15, \pm 10$ mm. Wire-mesh sensor signals were recorded after achieving a steady state for a measuring period of 10 s for each combination of boundary conditions. For each realized combination of superficial velocities data from both air and steam tests are available.

superficial water velocity (m/s) \ superficial gas velocity	0.0368	0.0574	0.0898	0.14	0.219	0.342	0.534	0.835
1.611	075	086	097	108	119	130	141	152
1.017	074	085	096	107	118	129	140	151
0.405	072	083	094	105	116	127	138	149
0.102	069	080	091	102	113	124	135	146

Fig. 5: Test matrix (grey: test points)

4. CFX pre-test calculations

Before the experiments were commissioned a pre-test calculation was set-up for the boundary conditions of the air-water test 074, which was performed at the superficial velocities $J_L = 1.0$ m/s and $J_G = 0.037$ m/s. Flow conditions correspond to the bubbly flow regime. For the CFD simulation with ANSYS CFX 10.0 the Eulerian two-phase flow model was used [8, 9], assuming that the gaseous phase consists of monodisperse bubbles with an pipe elevation dependent equivalent diameter of 4.8-5.2 mm in order to account for the hydrostatic bubble expansion. Both phases were treated as non-compressible. Bubble drag in accordance to Grace drag law, Tomiyama lift force, Frank's generalized wall lubrication force and the FAD turbulent dispersion force have been taken into account [10]. Bubble coalescence and fragmentation were neglected for this first pre-test simulation, also it can be assumed that bubble fragmentation will take place at the edges of the obstacle and coalescence might become of importance in regions of bubble accumulation i.e. in the wake behind the obstacle.

Steady state simulations with ANSYS CFX 10.0 were performed on two numerical meshes created with ICEM CFD Hexa and consisting of about 119.000 and 473.000 hexahedral mesh elements. Meshes were generated for half of the TOPFLOW geometry assuming axial symmetry. The flow domain for the CFD simulation consisted of 1.5 m pipe sections up- and downstream of the obstacle. Inlet boundary conditions were set to fully developed two-phase pipe flow profiles for air and water velocities, radial gas volume fraction distribution, turbulent kinetic energy and turbulent eddy frequency. At the outlet cross section of the 3.0 m long pipe section an averaged static pressure outlet boundary condition was used.

5. Experimental results

The sensor data was used to calculate two-dimensional time-averaged void fraction distributions in the measuring plane. By combining the information from measurements with different distances between sensor and diaphragm, full three-dimensional void distributions around the obstacle were obtained. A centre cut along the axis of the test pipe in a vertical plane perpendicular to the straight edge of the half-moon diaphragm is a very illustrative way to visualize the void fraction field. This was done in Fig. 6 for the field downstream of the diaphragm. At small superficial water velocities, there is a region free of bubbles directly behind the obstacle, which vanishes with growing water velocity. The wake, i.e. the zone where a distortion of the void field is found, grows in downstream direction with increasing liquid velocity, while the overall void fractions naturally decrease.

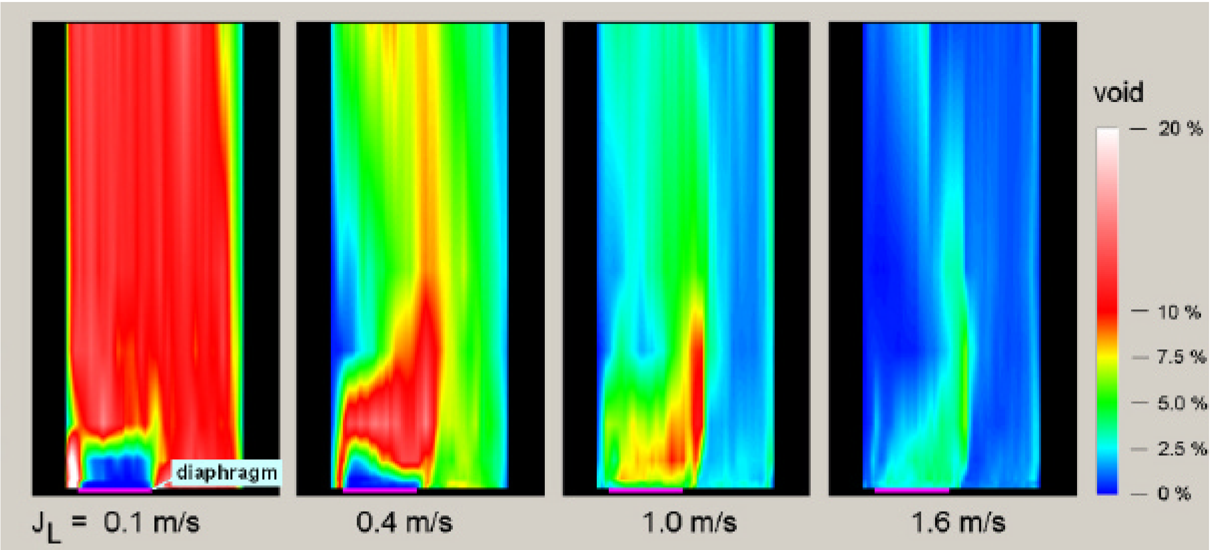

Fig. 6: Change of void fraction profiles downstream of the diaphragm at J_G = 0.037 m/s with a variation of the superficial liquid velocity J_L.

There is a way to assess time-averaged local liquid velocities by evaluating the transit time of bubbles of a certain range of diameters. Due to the spatial resolution, the sensor data can be used to determine the lateral extension of each individual bubble by measuring the maximum area occupied by the bubble within the measuring plane during its passage [2, 6]. If a spherical bubble shape can be assumed, the diameter of a circle with an equivalent area divided by the time of the passage reveals the bubble velocity. A local instantaneous value of the liquid velocity is available after subtracting the bubble rise velocity. Time-averaged profiles of the axial liquid velocity are calculated by averaging individual values from a manifold of analysed bubbles.
Bubble deformation causes a systematic error that has to be eliminated by a calibration procedure. In order to keep the bubble deformation and the bubble rise velocity in a narrow band, velocities are calculated only from bubbles of a certain bubble size interval, which was set to 4-5 mm, so-called "marker bubbles". It was assumed that the bubble deformation can be accounted for by a calibration factor of the individual bubble velocity. This factor is determined by integrating the velocity profile found under the assumption of spherical bubbles over the cross-section and comparing the result with the known liquid superficial velocity. Examples are shown in Fig. 7, where the results of both air and steam experiments executed at identical superficial velocities are shown.

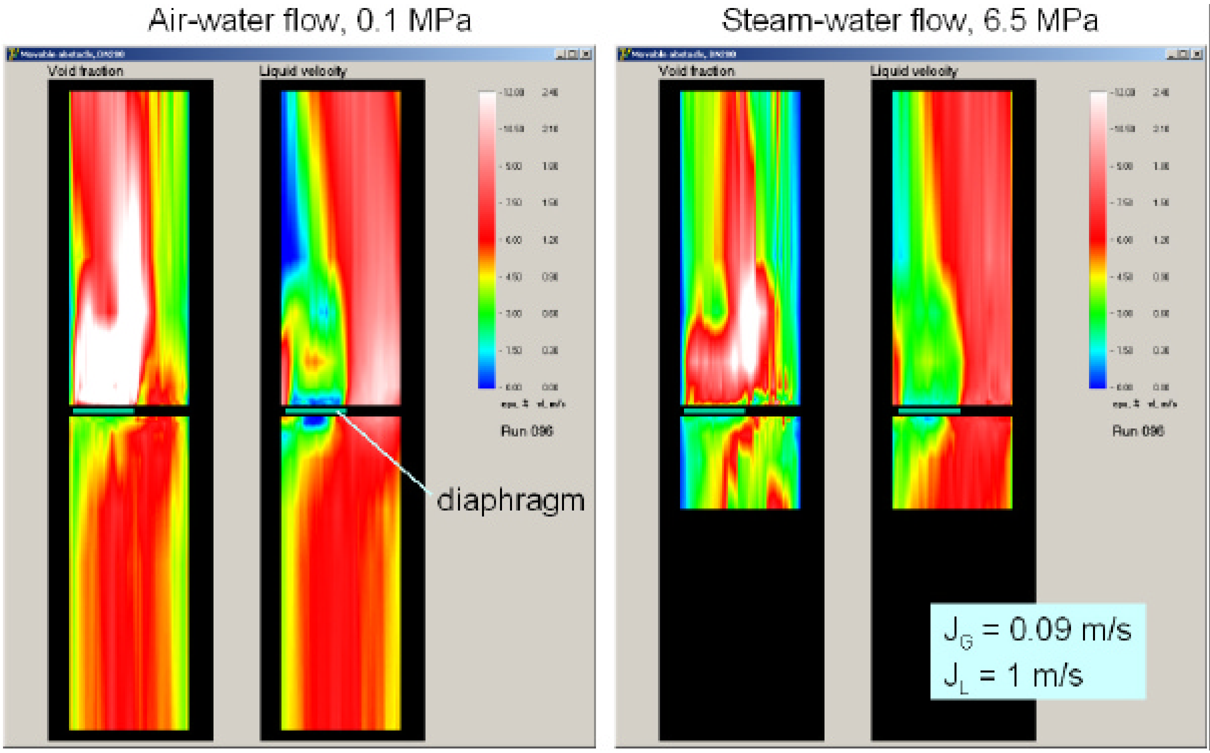

Fig. 7: Void fraction and liquid velocity profiles in an air-water and a steam-water test at identical superficial gas and liquid velocities.

The velocity field indicates a recirculation zone behind the obstacle. It has to be kept in mind that the marker bubble method cannot supply information on the sign of the axial liquid velocity. Negative values expected in the centre of the recirculation zone can therefore not be reproduced and a local maximum is found instead.
By the estimation of liquid velocity profiles it becomes clear that the high gas fractions in the wake of the obstacle are caused by entrapping bubbles in the recirculation zone. On the other hand, upstream of the diaphragm the expected stagnation point is nicely reproduced and the concentration of the gaseous phase is decreased. In the free cross-section area aside of the obstacle both velocity and gas fraction show maxima.
Concerning the general structure of the two-phase flow field, no large qualitative differences were found between the air-water and the steam-water experiment. The void fractions and the velocities are smaller in case of the high-pressure tests. The recirculation zone is less pronounced.

6. Result of the ANSYS CFX pre-test calculation

The steady-state ANSYS CFX calculations have well reproduced all details of the structure of the two-phase flow field around the diaphragm for test conditions of TOPFLOW-074 (Fig. 8). This concerns shape and extension of the recirculation area, the stagnation zone upstream of the diaphragm as well as the velocity and void fraction maxima in the non-obstructed part of the cross-section. Smaller details, like the velocity and void fraction maxima above the gap between the circular edge of the obstacle and the inner wall of the pipe are also found in a good agreement between experiment and calculation.
The 3-dimensional dataset from wire-mesh sensor measurements has been imported into the CFX graphical postprocessor in order to allow for the application of identical data processing, color schemes and therefore a more direct comparison of the CFD results and experimental data. Since experimental data have a fine (64×64) planar resolution in the x-y-plane but a limited coarser resolution in z-direction with respect to measuring planes, a pre-interpolation of the experimental data in z-direction has been applied with an axial resolution of the interpolated data with Δz=1mm.

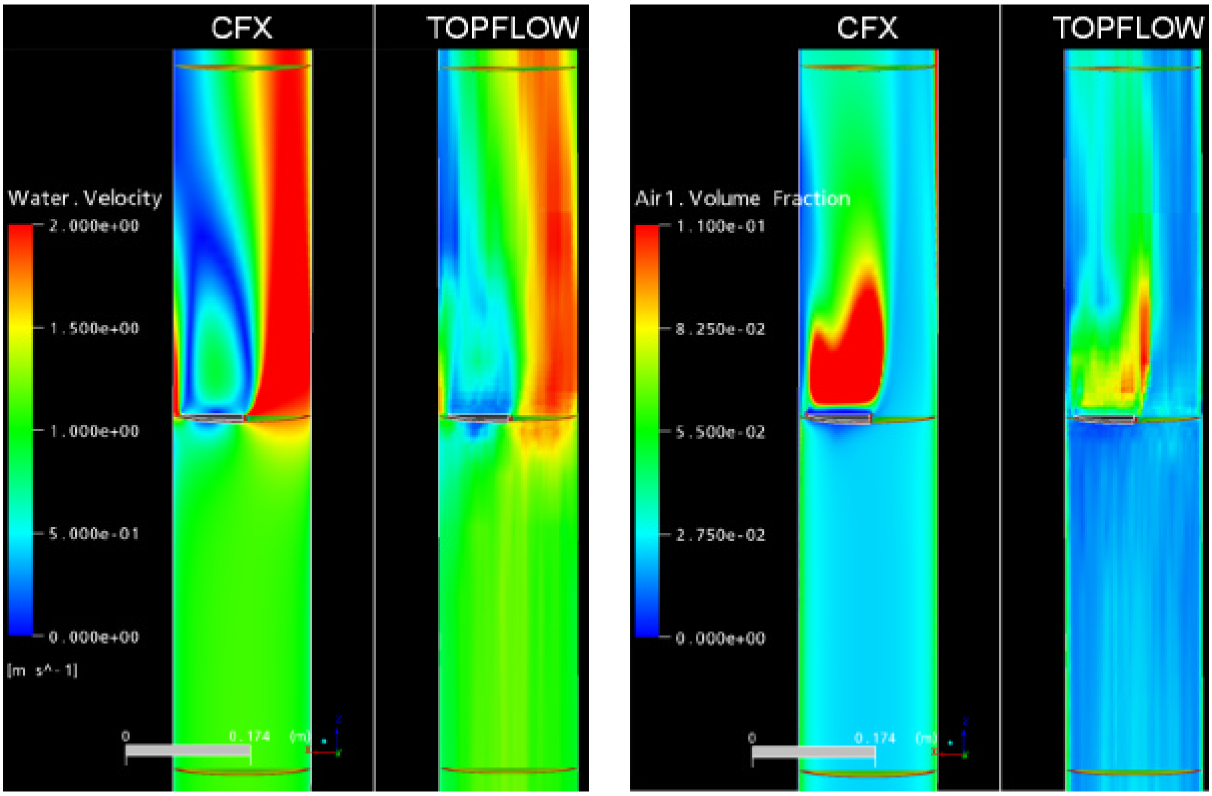

Fig. 8: Comparison between experiment and CFX pre-test calculation for the absolute water velocities (left) and the gas volume fraction distribution (right) for the region from 0.5 m upstream to 0.5 m downstream the obstacle; air-water test at J_L=1 m/s and J_G=0.037 m/s.

Results of the comparison of ANSYS CFX pre-test calculations on the finer grid with measurement data are shown in Fig. 8 for absolute water velocity and gas volume fraction distributions. The velocity field behind the obstacle shows the same location and intensity of the recirculation zone and stagnation regions on the obstacle surface. The reattachment length of the flow to the pipe wall downstream the obstacle is slightly increased in the CFD simulation, which is probably linked to the higher amount of entrained gas void fraction in the vortex behind the obstacle. Furthermore the present simulation tends to overpredict the void fractions in the wake. This is a result of the assumption of a mono-disperse bubbly flow with a bubble size differing from reality and neglecting bubble coalescence with formation of larger bubbles in the wake of the obstacle. The agreement can be improved by using measured bubble-size distributions from the region upstream of the obstacle as a boundary condition for post-test calculations or by application of the inhomogeneous MUSIG model for the prediction of bubble size distributions from local flow conditions.

7. Conclusions

A novel technique to study the two-phase flow field around an asymmetric diaphragm in a vertical pipe is presented, that allows to produce data for CFD code validation in complex geometries. Main feature is a translocation of the diaphragm to scan the 3D void field with a stationary wire-mesh sensor. Besides time-averaged void fraction fields, a novel data evaluation method was developed to extract estimated liquid velocity profiles from the wire-mesh sensor data.
The flow around an obstacle of the chosen geometry has many topological similarities with complex flow situations in bends, T-juctions, valves, safety valves and other components of power plant equipment and flow phenomena like curved stream lines, which form significant angles with the gravity vector, flow separation at sharp edges and recirculation zones in their wake are present. It is the goal of the ongoing CFD code development to accurately model such phenomena in a two-phase flow. Therefore, the experiments provide a good basis for the test and the validation of the codes and their underlying multiphase flow and turbulence models. Due to the generalizing

capability of CFD codes, that can adapt to different geometric boundary conditions by the mesh generation, a successful validation on the kind of obtained experimental data guarantees the applicability of the code to other equally complex flow fields.
A pre-test calculation done by ANSYS CFX 10.0 resulted in a good agreement with the experiment in terms of all significant qualitative details of the void fraction and velocity distributions. The structure and the geometry of the entire flow field in general as well as the dimensions of recirculation and stagnation zones in particular were predicted in good agreement with the experiment. The fact that for the time being a simple monodispers bubbly flow was assumed, lead to an overestimation of void fractions especially in the wake of the obstacle, while the velocity profiles are matching better. It is planned to continue with post-test calculations in order to achieve a better quantitative agreement by using measured bubble-size distributions from the region upstream of the obstacle as inlet boundary condition and in a further step by applying the inhomogeneous MUSIG model for the prediction of bubble size distribution and bubble coalescence. The experimental data will be used to validate this recently developed and implemented model against detailed bubble size and bubble scale resolved void fraction measurements.

References

[1] A. Schaffrath, A.-K. Krüssenberg, F.-P. Weiss, E. F. Hicken, M. Beyer, H. Carl, J. Schuster, P. Schuetz, M. Tamme, 2001, TOPFLOW - a new multipurpose thermalhydraulic test facility for the investigation of steady state and transient two-phase flow phenomena, Kerntechnik, **66**(2001)4, pp. 209-212.

[2] Prasser, H.-M., Beyer, M., Böttger, A., Carl, H., Lucas, D., Schaffrath, A., Schütz, P., Weiss, F.-P., Zschau, J.: Influence of the pipe diameter on the structure of the gas-liquid interface in a vertical two-phase pipe flow, Nuclear Technology 152 (2005) 10. pp. 3-22.

[3] H.-M. Prasser, M. Beyer, A. Böttger, H. Carl, D. Lucas, A. Schaffrath, P. Schütz, F.-P. Weiß, J. Zschau, TOPFLOW Tests on the Structure of the Gas-Liquid Interface in a Large Vertical Pipe, Jahrestagung Kerntechnik 2004, Düsseldorf, 25.-27. Mai 2004, pp. 69 - 74.

[4] H.-M. Prasser, Influence of the Gas Injection on the Void Fraction Profiles and Bubble Size Distributions of a Air-Water Flow in Vertical Pipes, 5th ICMF'04, Yokohama, Japan, May 30–June 4, 2004, #187.

[5] H.-M. Prasser, M. Beyer, H. Carl, H. Pietruske, P. Schütz: Steam-water experiments at high pressure to study the structure of the gas-liquid interface in a large vertical pipe, Annual Meeting on Nuclear Technology, Nuremberg, May 10-12, 2005, paper 215.

[6] H. Pietruske, H.-M. Prasser: Wire-mesh sensors for high-resolving two-phase flow studies at high pressures and temperatures, NURETH-11, Avignon, France, Oct. 2-6, 2005, #533.

[7] H.-M. Prasser, D. Scholz, C. Zippe, 2001, Bubble size measurement using wire-mesh sensors, Flow Measurement and Instrumentation, 12/4, pp.299-312, 2001.

[8] ANSYS CFX 10.0 Users Manual, ANSYS Inc., July 2005.

[9] Th. Frank, J. Shi, A.D. Burns: "Validation of Eulerian multiphase flow models for nuclear reactor safety applications", 3rd TPFMI, Pisa, 22.-24. Sept. 2004, pp. 1-8.

[10] Th. Frank: Abschlussbericht zum Forschungsvorhaben 150 1271 "Entwicklung von CFD-Software zur Simulation mehrdimensionaler Strömungen im Reaktorkühlsystem", ANSYS Germany, Technical Report TR-06-01, Januar 2006, pp. 1-72.

Acknowledgements

The work is carried out is part of current research projects funded by the German Federal Ministry of Economics and Labour, project numbers 150 1265 and 150 1271. Electronic equipment for wire-mesh sensors was developed in co-operation with TELETRONIC GmbH (www.tz-rotech.de/teletronic/). The authors express their gratitude to the technical TOPFLOW team.